Coupling Low-Voltage Microgrids into Mid-Voltage Distribution Systems

Zhao Wang*

University of Notre Dame, Notre Dame, IN, 46556, US

This report presents results of the first two stages of the project, i.e. algorithm development and simulation model development. A hierarchical control architecture is proposed to achieve the objective of exporting maximum real power to mid-voltage (MV) distribution network by coupling low-voltage (LV) microgrids. At the same time, reactive power is dispatched in a coordinated way so that regulatory constraints on voltage are satisfied. Two levels of optimization problems are solved to determine set points of each microsource controller. Corresponding simulation model is developed in MATLAB® Simulink® with SimPowerSystems™ toolbox. Simulation results show that the algorithm developed can maintain system stability, while simultaneously achieving the goal of maximizing real power export under voltage regulation constraints.

Nomenclature

$S = P + jQ$	Complex Power, with Real Power P and Reactive Power Q
$Z = R + jX$	Impedance, with Resistance R and Reactance X
$Y = G + jB$	Admittance, with Conductance G and Susceptance B
$E\angle\delta$	Bus Voltage Phasor, with Magnitude E and Phase Angle δ
m_P	$P - f$ Droop Controller Parameter
m_Q	$Q - E$ Droop Controller Parameter
Subscript	
i	Bus number
gen	Power Generation
ln	Distribution line
ms	Microsource

*Graduate Student, Department of Electrical Engineering.

I. Introduction

A. Challenges in Future Power Grid

The power grid system is expected to see tremendous changes, both in its infrastructure and the way it operates. One of the most significant changes is expected due to a high level penetration of distributed energy resources (DERs), especially in LV distribution networks. As shown in figure 1, there would be a large amount of renewable energy resources in the future power grid. Besides the wind farms and solar farms directly connected to the high-voltage (HV) transmission networks, renewable energy resources will also locate throughout the distribution network in the form of DERs, such as roof-top solar panels.

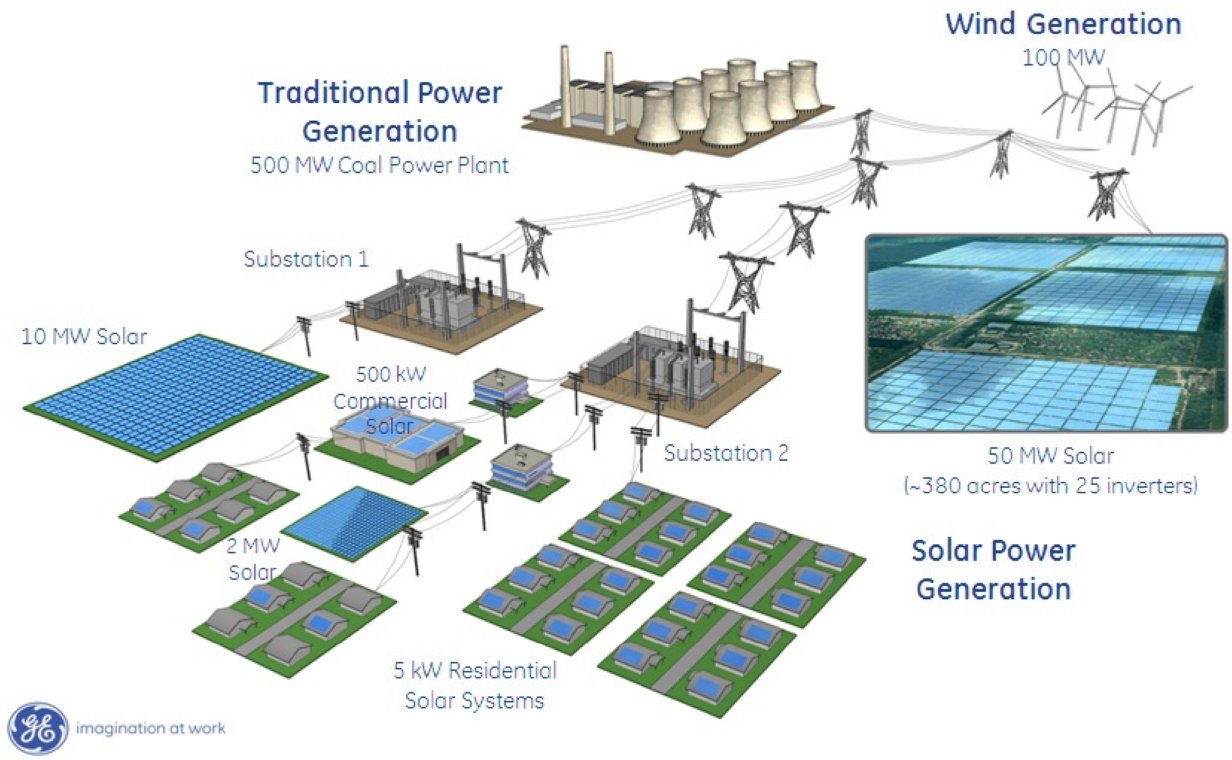

Figure 1. Future power grid from GE's perspective

DERs are promoted as a means to meet the constantly increasing demand for high quality electric power. DERs are distributed throughout the entire network, near the end customers. The DER concept works with a wide range of energy resources, such as diesel engine generator, micro-turbine, wind turbine, solar panel, as well as storage devices and controllable loads.

The introduction of DER's, however, may cause as many problems as it can solve.[1] Some problem arises from the multi-directional power flows that occur, when integrated DERs export real power back to the grid. Currently, power is generated from centralized power plants, going through transmission lines, substations, distribution feeders, and finally delivered to end customers. Both control methods and protection mechanisms are inherently designed to work in a one-directional manner from generation to end user. Since DERs are coupled into the distribution network, the high penetration of DER's may result in power flow that move in the opposite direction to conventional flow situation. This results in the "voltage rise problem".

The so called "voltage rise problem" happens when DERs try to export real power back to the distribution network. Because of the weakness of LV and MV segments of the power grid, this problem is much more severe in these networks than in the high-voltage (HV) transmission network. As a result, we need to formulate and solve the voltage regulation problem assuming weak LV and MV distribution networks.

Frequency and voltage magnitude are important indicators of power quality and reliability in the grid. Further integration of DERs is not appropriate unless the voltage rise problem is solved. Accordingly, this report examines control algorithms that maximize real power export, while maintaining the voltage profile within limits, respecting constraints on MV line capacity and DERs' generation capabilities.

B. Distribution System Architecture

We are interested in a distribution system with radial structure. As illustrated in figure 2, a long MV distribution line ties to one single primary substation, and all buses distribute along the line. This represents a typical rural distribution network with all of its customers tied to a single line. Although power flow relationships are relatively simple, the voltage rise phenomenon is more substantial with this architecture.[2] This network will be a running example used throughout the report.

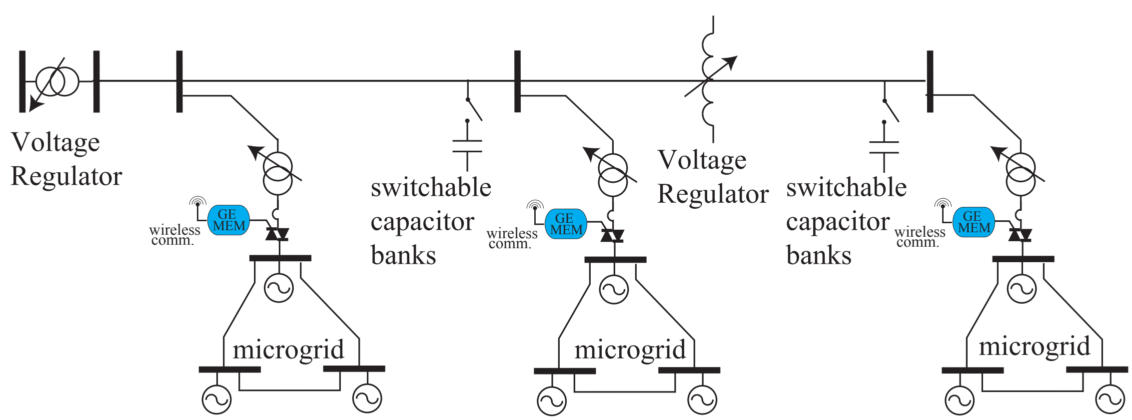

Figure 2. Distribution system control architecture

In order to discuss controls in such a distribution system, we need further assumptions about this network on the control we can apply. As shown in figure 2, a microgrid or pure load is connected to each downstream bus. If microgrids are connected, a controller is located at the point of common coupling (PCC) between the microgrid and the network. The controller maintains set point at the PCC, and coordinates with neighboring agents to achieve a common objective.

Legacy control devices and protection mechanisms exist in the system as well, hence we have to ensure the compatibility of our control algorithm with these legacy devices. These legacy control devices are switchable capacitor/inductor banks, voltage regulators (VRs), and static var compensators (SVCs).

C. Objective and Approach

The objective of our work is to maximize the real power exported back to the MV distribution network from coupled LV microgrids. The constraints considered include regulatory constraints on voltage magnitude and frequency, transient stability in the face of faults, topology variations, or set point changes, as well as compatibility with legacy control devices on the MV distribution network.

A multi-layer hierarchical control architecture is proposed, as shown in figure 3. At the bottom level of the hierarchical structure, we have microsource controllers tied to DERs within microgrids. These controllers ensure the multi-unit stability of the network for a selected set point provided by upper level microgrid controllers. At the PCC, we have a microgrid interface controller (MIC). The MIC of a microgrid designates a set point to each microsource controller satisfying the real power and voltage level demanded by the top-level supervisor. The supervisor is called the microgrid consortium manager (MCM). It determines a set point for each MIC that maximizes the real power export subject to constraints on voltage, frequency, and MV line capacity.

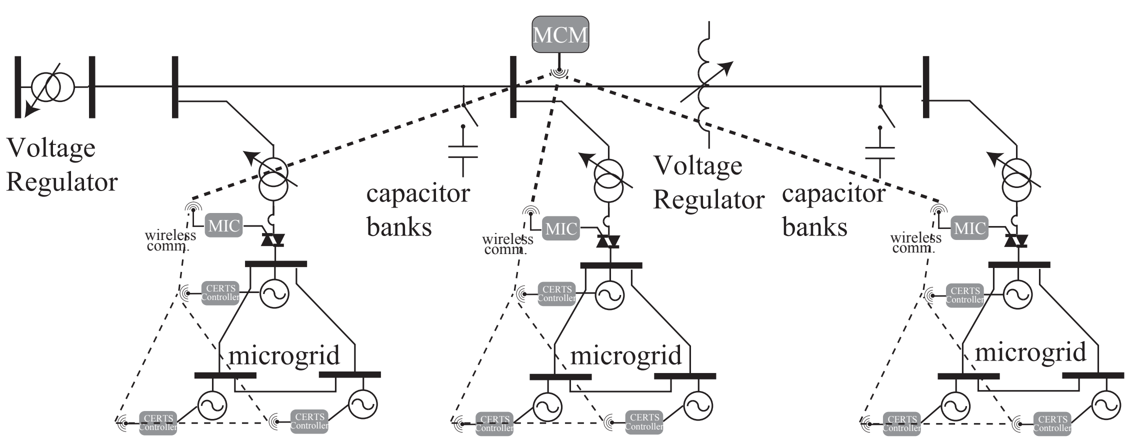

Figure 3. Complete system model of hierarchical system

The proposed algorithm has several potential benefits. First, by maximizing real power export from the coupled microgrids, we can increase the profit of operating such a LV microgrid, hence making integration of DERs more favorable from the microgrid operators' perspectives. Second, since the algorithm must be compatible with legacy controls, the impact of this method on a DSO's voltage regulation policies is minimized. This would encourage the higher penetration of DER from DSO's point of view.

Coupled microgrids not only provide real power service but they can also be used for voltage control in the distribution network. Voltage control is a kind of "ancillary services" that must be provided with the transaction of power service. Ancillary services are crucial for maintaining reliable operation of the power grid. Besides voltage control service, one can also provide load following, operating reserves, and energy imbalance with the same control system we present here. Then coupled microgrids would become a more active player in both power service and ancillary service markets.

D. Report Outline

The remainder of this report is organized as follows. Section II describes the distribution system under study and provides details on the system model. Section III explains how the voltage rise problem occurs. Section IV presents the hierarchical control system in detail, and shows the optimization problems solved by both MIC and MCM. Section V introduces the simulation models used to study the control algorithm's performances, and shows the simulation results. Section VI discusses conclusion and future work.

II. System Model

This section provides a detailed description of the radial system model, as well as specifications and assumptions used in our algorithm development, simulation, and verification processes. The Droop control concept is introduced as a fundamental element of our hierarchical control system. Based on this concept, the CERTS droop controller is discussed, especially its structure and distributed nature.[5] The CERTS droop controller is capable of stabilizing the distribution network.

A. System Model of the Distribution Network

Considering the hierarchical control architecture given in Section I, there are two layers of network model corresponding to both MCM and MICs. The network for the MCM is shown in figure 4. There are N buses in this network. Bus 1 is connected to the primary substation, hence represents the main grid. Microgrids or pure loads connected to the remaining $N-1$ buses are modeled as a microsource and a load tied to each bus. This modification is appropriate, because microgrids keep real and reactive power levels during operation.

Voltage magnitude and phase angle of bus i are E_i and δ_i. Specifically, bus 1 has $E_1 = 1.0$ pu and $\delta_1 = 0°$. Real and reactive power injected through bus i into the network are P_i and Q_i. Signs of P_i and Q_i represent the direction of power flows, and a positive sign means power injection into the network.

The microgrid controlled by the MICs is shown in figure 5. There are M buses in this microgrid. Bus 1 is connected to the PCC, and represents the input/output port of the microgrid. A microsource and a load

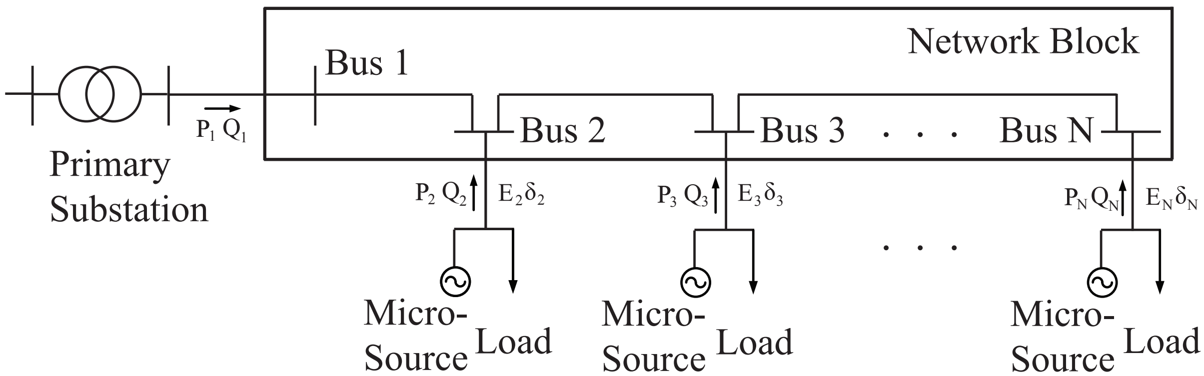

Figure 4. System model MCM

are connected to each of the remaining $M-1$ buses.

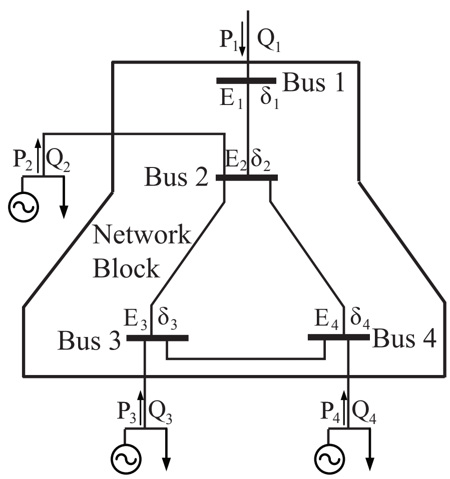

Figure 5. System model MIC

Voltage magnitude and phase angle of bus i are E_i and δ_i. Real and reactive power injected through bus i into the network are P_i and Q_i. Signs of P_i and Q_i represent the direction of power flows, and a positive sign means power injection into the microgrid. Specifically, bus 1 has $E_1 = E_i^*$ and $P_1 = -P_i^*$, i.e. the set point given by MCM to the MIC.

To express the real power loss P_{loss} over the lines, we define the "network block" in figure 4 and figure 5. The "network block" only incorporates distribution lines connecting all the buses. Because the block has no generation capability, it is a passive system, only capable of consuming power. This definition helps when we consider the total line loss in our optimization problem. The real power loss is the sum of real power injection into the network over all buses $P_{loss} = \sum P_i$.

Specifications of distribution lines is another very important aspect of our modeling. In contrast to HV transmission lines, LV and MV distribution lines have a nontrivial ratio of $\frac{R}{X}$, where R is line resistance and X is line reactance. This type of network is usually called a "weak network", indicating its vulnerability to disturbances. In our analysis and algorithm development, we consider weak systems with coupled real and reactive power control.

B. Droop Control Concept

For each microsource connected to the network, droop control schemes are employed to maintain a given set point. The set point for bus i includes both real power P_i^* and voltage E_i^*. The droop controller is a conventional grid control concept that has been applied to low voltage grids.[6] The two forms of droop control are the reactive power-voltage $(Q - E)$ droop and the real power-frequency $(P - f)$ droop, both illustrated in figure 6. Droop control scheme is distributed by its nature, because it determines control inputs only based on local measurements. Simulation results show that droop controllers maintain system stability under disturbances.

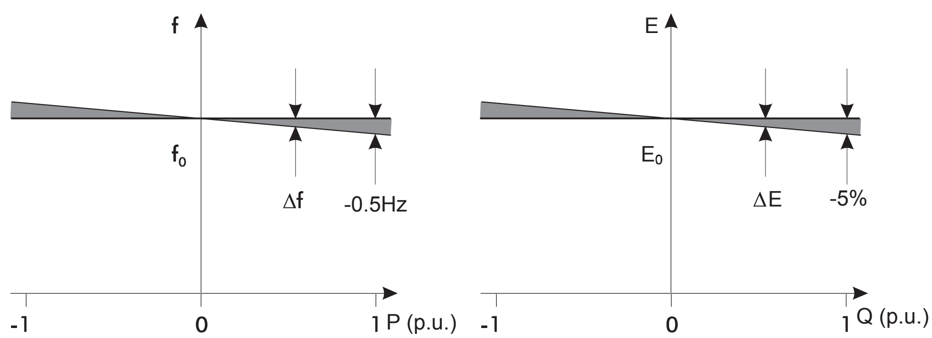

Figure 6. P-f and Q-E Droops

To maintain set points, the regulation procedure of droop controllers closes a feedback loop. For example, P-f droop in figure 6 works as follows. In a power system, nominal real power and frequency are set to be 0 pu and f_0 respectively, which means frequency is maintained by strictly ensuring real power balance. If some bus in the network loses generation capacity, then frequency of the network drops by $\triangle f$. Measuring this frequency change, other droop controllers react by increasing the real power injection into the network from other buses by $\triangle P$ that is proportional to $\triangle f$. With increased real power contribution from these droop controllers, the network reaches a new balance. Similarly, reactive power balance within the network is maintained through Q-E droop. As a result, these droop controllers ensure both frequency and voltage stability of a distribution network.

C. CERTS Droop Controller Structure

For voltage control, the Q-E droop controller used here is:

$$\dot{E}_i = (E_i^0 - E_i) - m_Q Q_i, \tag{1}$$

where E_i^0 is the requested voltage level, and m_Q is the $Q - E$ droop parameter chosen to meet specified performance. For example, with $m_Q = 0.05$, we accept 0.05 pu voltage magnitude change corresponding to 1 pu of reactive power support.

For frequency synchronization, we consider the following P-f droop controller:

$$\dot{\delta}_i = m_P(P_i^0 - P_i), \tag{2}$$

where P_i^0 is the requested active power. Similarly, with $m_P = \pi$, we allow $\frac{\pi}{2\pi} = 0.5\ Hz$ frequency change due to 1 pu of real power variation.

The stability of these controller structures have been verified through a simulation of a microgrid testbed at University of Wisconsin-Madison.[1] The structure of the microsource controller is shown in figure 7. Those features of the controller that help to ensure controller stability are low pass filters used to reduce the propagation of noise inherent in the network and attenuate 120Hz ripples during unbalanced operation, as well as voltage control block added to the traditional $Q - E$ droop controller to obtain the controller equation (1).

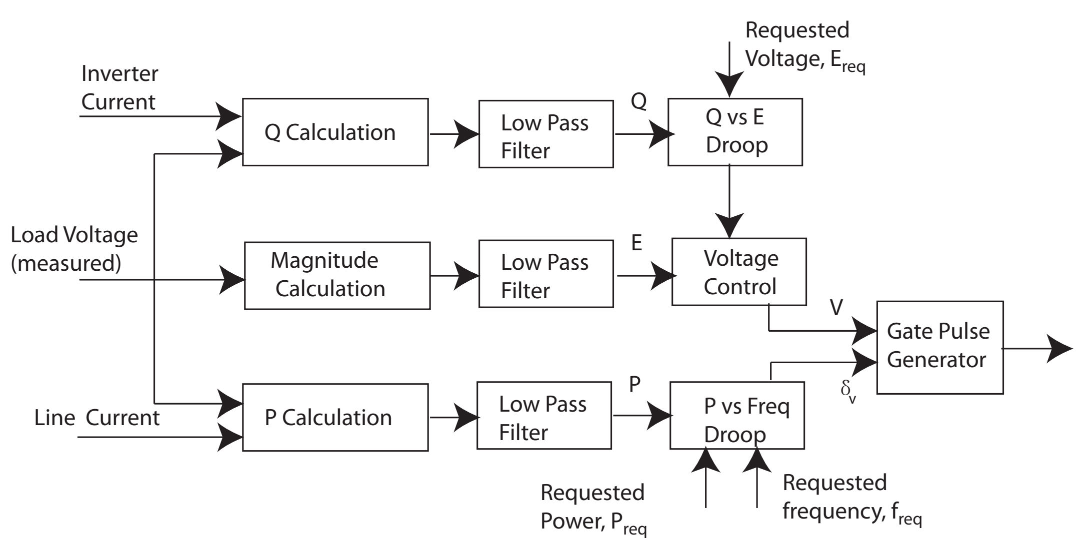

Figure 7. Block Diagram of CERTS Micro-grid Droop Controller

Integration of the droop controller with inverter is shown in figure 8. This inverter interfaces to any distributed generation (DG) unit. The power generated by DG is buffered by a storage device, such as the ultracapacitor in figure 8. The DC power stored at the buffer is then transformed to three-phase AC power. The controller measures the inverter's output real power and voltage, compares them with set points given by upper level MICs, then modulates frequency and reactive power to maintain them.

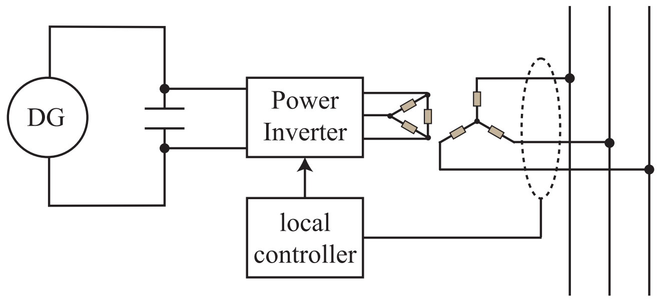

Figure 8. Inverter structure

To realize communication with higher level controller, a dispatcher is attached to the controller discussed above, as shown in figure 9. Actually, the dispatcher designates set points to the controller to achieve optimal operation.

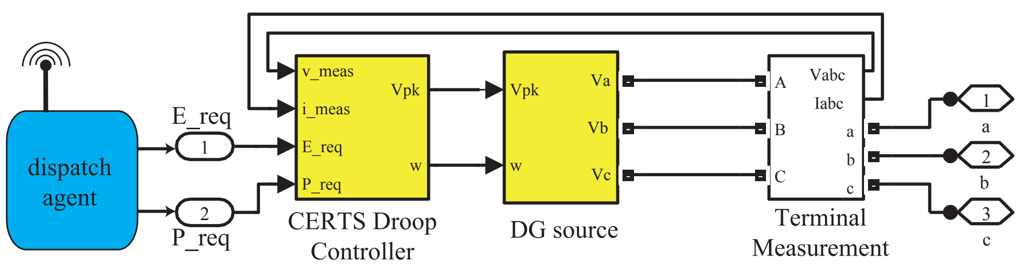

Figure 9. Realization of controller

With CERTS droop controllers connected to microsources, we can form a microgrid to provide higher quality power services to customers. A single microgrid with both generation and load was simulated with SimPowerSystems™ toolbox in Simulink®. This model was validated against hardware tests at the University of Wisconsin-Madison. The tests show that the controller kept the stable operation in this simulation model through events such as islanding, losing generation capacity, load shedding, and generator reconnection.

III. Voltage Rise Problem

This section explains the voltage rise problem with a phasor diagram and an example using our system model. From the same phasor diagram, a solution to this problem is derived, and the resultant example model system is given subsequently. At the end, a comparison between reactive power control and voltage control is discussed.

A. Explanation of Voltage Rise Problem

To explain the voltage rise problem, we work with the circuit model in figure 10. In this two-port single-line circuit, one port is connected to the primary substation and the voltage is kept to $V_0\angle 0°$ as reference. The other side is connected to a generator, trying to inject a complex power $S_E = P_E + jQ_E$ with a terminal voltage of $E\angle\delta$. The distribution line impedance is $Z = R + jX$, where R is the resistance and X is the reactance. The current going through the line is $I\angle\phi$, which is from the generator to the primary substation.

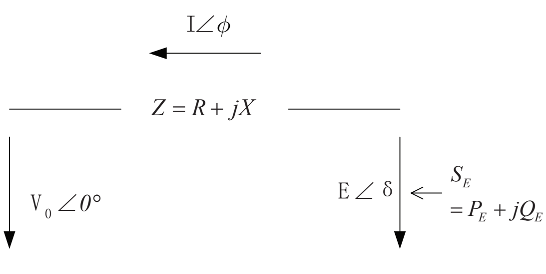

Figure 10. Simple circuit model to illustrate voltage rise problem

Initially, we assume no reactive power support is provided when the generator exports real power, i.e. $P_E > 0$ and $Q_E = 0$. Based on the vector relationship of these variables, we can obtain the phasor diagram of this circuit as shown in figure 11.

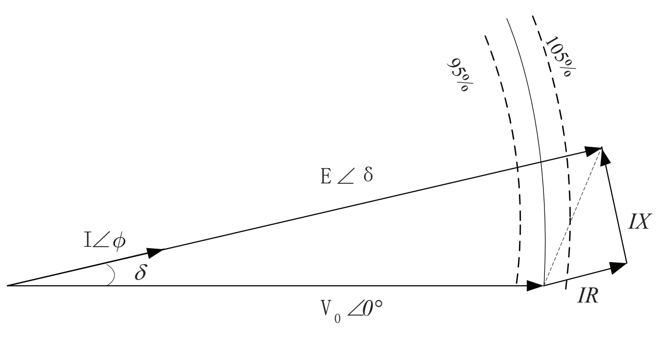

Figure 11. Phasor diagram of voltage rise problem

This figure shows that, with zero reactive power support, the current phasor aligns with the terminal voltage phasor. Considering the voltage over the distribution line, the result violates the regulatory constraint requiring voltage magnitude to lie within ±5% of the nominal value.

For the distribution network shown in Section II, we illustrate how the voltage rise problem occurs when real power is injected through downstream buses. Without loss of generality, let the farthest bus inject real power without providing any reactive power support. Figure 12 shows the voltage profile when $20kW$, $100kW$, and $200kW$ real power are injected into the network. The figure shows that when only $20kW$ is exported from bus 5, all bus voltages retain within voltage limits. When, however, the amount of real power injected increases to $100kW$ or $200kW$, the regulatory voltage limits are violated.

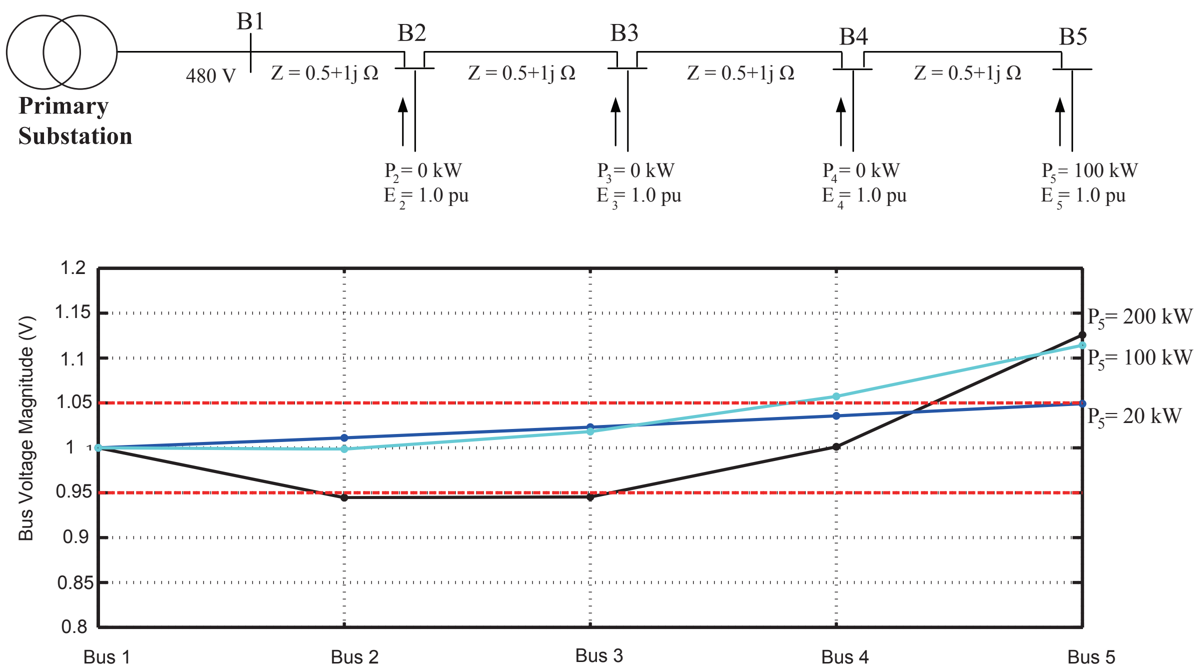

Figure 12. Example of voltage rise problem

B. Solution to Voltage Rise Problem

We can use the same circuit model and phasor diagram to find a solution to the voltage rise problem. In the previous phasor diagram in figure 11, we let the current vector $I\angle\phi$ lead the voltage vector $E\angle\delta$ to reduce the magnitude of the resultant terminal voltage. The corresponding phasor diagram in figure 13 shows that the voltage over the distribution line rotates counterclockwise. This rotation of the current phasor reduces the terminal voltage to be within limits marked by dashed curves.

With current vector leading voltage vector, we have a negative phase angle difference $(\delta - \phi)$. The complex power injected by the generator satisfies $S_E = P_E + jQ_E = EI\angle(\delta - \phi)$, hence $Q_E = EIsin(\delta - \phi)$ < 0. This means that, instead of exporting reactive power, the generator must absorb it at the terminal

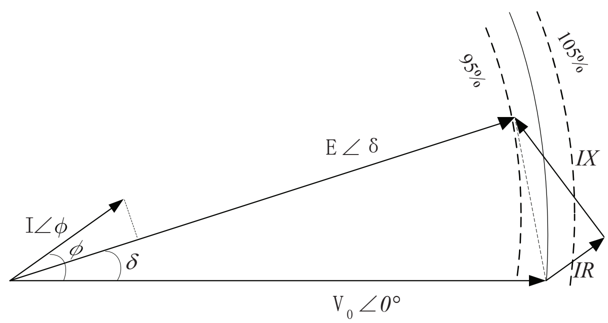

Figure 13. Phasor diagram of solution to voltage rise problem

port. As a result, the solution is to provide reactive power support at the point of real power export. In distribution networks, reactive power support is provided by switchable capacitor/inductor banks, static var compensators, and also microgrids controlled by Q-E droops.

Using the example distribution network, one shows that the reactive power control maintains the system voltage profile within regulatory limits. For the same network, instead of maintaining real and reactive power at each bus, we let it keep real power and voltage set points. Assuming that $100kW$ of real power is injected into the network, one can derive the required reactive power support at each bus. This is shown in figure 14. Several remarks should be made here: i) the amount of required reactive power support may exceed the physical limits of equipments' generation capabilities; ii) except at the bus of real power injection, which should consume reactive power, other buses must export it into the network; iii) the provision of reactive power support must be coordinated to maintain voltage profile within the network.

C. Reactive Power Control v.s. Voltage Control

In order to reduce the resultant terminal voltage, we can either directly change its magnitude or control reactive power flows. Directly changing voltage magnitude is achieved using voltage regulators through changing tap position of the output coil. This approach may not be available because voltage regulators have a limited number of control steps and low control bandwidths. In contrast, the reactive power control can be fully provided by the coupled microgrids. So the method we implement is to coordinate coupled LV microgrids to export maximum real power while providing reactive power support, thereby maintaining a voltage profile conforming to regulatory constraints.

IV. Control Architecture

The hierarchical control system structure consists of low-level CERTS droop controllers, mid-level MICs, and a high-level MCM, as shown in figure 3. CERTS droop controllers have been discussed in Section II.

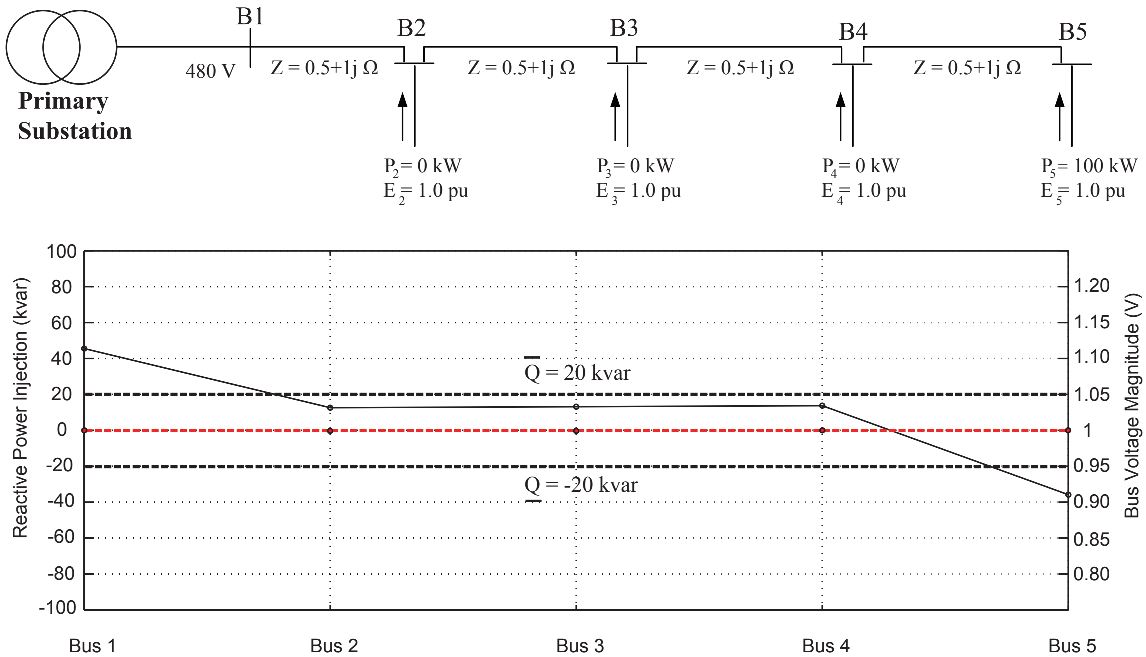

Figure 14. Example of solution to voltage rise problem

The MIC and MCM control algorithms are considered in this section.

A. Microgrid Interface Controller

The MIC maintains the set point given by the MCM, and determines set points of the microsources within its microgrid. Determination of the set points is achieved by solving an optimization problem, which aims to minimize microgrid running cost.

The objective of the MIC optimization problem is to minimize the generation costs while maintaining the given set point at the PCC. The optimization is done subject to constraints on microsource generation capacities, LV line power flow limits, regulatory constraint on voltage and frequency, and the set point at the PCC. Solutions to this problem are the real power and voltage set points, as introduced in Section II. These set points are directly fed to the CERTS droop controllers as inputs. Assuming there are M buses and L lines connecting them, this optimization problem is expressed as:

$$\begin{aligned} &Minimize && C\left(\sum_{i=2}^{M} P_{ms,i}\right) \\ &w.r.t. && E_i \quad P_{ms,i} \quad (i = 2, 3, \cdots, M) \\ &subject \quad to && Generation \quad Capability \quad Constraints \quad (i = 2, 3, \cdots, M) \\ & && \underline{P_{ms,i}} \leq P_{ms,i} \leq \overline{P_{ms,i}} \end{aligned}$$

$$
\begin{aligned}
& \underline{Q_{ms,i}} \leq Q_{ms,i} \leq \overline{Q_{ms,i}} \\
& Power \quad Flow \quad Constraints \quad (i = 1, 2, \cdots, L) \\
& \underline{P_{ln,i}} \leq P_{ln,i} \leq \overline{P_{ln,i}} \\
& \underline{Q_{ln,i}} \leq Q_{ln,i} \leq \overline{Q_{ln,i}} \\
& Voltage \quad Regulation \quad Rule \quad (i = 2, 3, \cdots, M) \\
& \underline{E_i} \leq E_i \leq \overline{E_i} \\
& Power \quad Balance \quad Relationship \quad (i = 1, 2, \cdots, M) \\
P_i \quad = \quad & E_i \sum E_j \left(G_{BUS,ij} \cos(\delta_i - \delta_j) + B_{BUS,ij} \sin(\delta_i - \delta_j) \right) \\
P_i \quad = \quad & P_{ms,i} - P_{load,i} \\
Q_i \quad = \quad & E_i \sum E_j \left(G_{BUS,ij} \sin(\delta_i - \delta_j) - B_{BUS,ij} \cos(\delta_i - \delta_j) \right) \\
Q_i \quad = \quad & Q_{ms,i} - Q_{load,i}
\end{aligned}
$$

where $C(\cdot)$ is the cost function of running the microgrid, primarily the cost of power generation.

Every time a microgrid's topology or parameters change, its MIC must recalculate set points for lower level CERTS controllers. With the new set points, the real power and voltage settings are kept unchanged at the PCC. If the capacity of the entire microgrid varies, then it must inform the higher level MCM to recalculate a set point with respect to this new constraint.

Since the microgrid concept deals with microsources in close proximity, we can operate a communication network to transmit set points and to update any change concerning microgrid topology and parameters. This optimization problem is solved numerically in a centralized fashion, and set points are transmitted locally through a wireless communication network.

B. Microgrid Consortium Manager

The MCM determines set points for MICs, in order to maximize real power export while maintaining voltage profile within regulatory limits.

The objective of this optimization problem is to maximize real power export through the primary substation. This problem is equivalent to minimizing the amount of real power generation capacity not used and the amount of real power lost along the distribution lines. Combining the two parts together, the objective function is simplified to P_1, i.e. the real power exported through the primary substation to the main grid. Solutions to this problem are sent to the MICs as set points. Assuming there are N buses and $N-1$ lines connecting them, the optimization problem is expressed as:

$$
\begin{aligned}
Minimize \quad & E_1 \sum_{j=1}^{N} E_j \left(G_{BUS,1j} \cos(\delta_1 - \delta_j) + B_{BUS,1j} \sin(\delta_1 - \delta_j) \right) \\
w.r.t. \quad & E_i \quad P_i \quad (i = 2, 3, \cdots, N) \\
subject \quad to \quad & Generation \quad Capability \quad Constraints \quad (i = 2, 3, \cdots, N) \\
& \underline{P_{gen,i}} \leq P_{gen,i} \leq \overline{P_{gen,i}} \\
& \underline{Q_{gen,i}} \leq Q_{gen,i} \leq \overline{Q_{gen,i}} \\
& Power \quad Flow \quad Constraints \quad (i = 1, 2, \cdots, N-1) \\
& \underline{P_{ln,i}} \leq P_{ln,i} \leq \overline{P_{ln,i}} \\
& \underline{Q_{ln,i}} \leq Q_{ln,i} \leq \overline{Q_{ln,i}} \\
& Voltage \quad Regulation \quad Rule \quad (i = 2, 3, \cdots, N) \\
& \underline{E_i} \leq E_i \leq \overline{E_i} \\
& Power \quad Balance \quad Relationship \quad (i = 1, 2, \cdots, N) \\
P_i \quad = \quad & E_i \sum E_j \left(G_{BUS,ij} \cos(\delta_i - \delta_j) + B_{BUS,ij} \sin(\delta_i - \delta_j) \right) \\
Q_i \quad = \quad & E_i \sum E_j \left(G_{BUS,ij} \sin(\delta_i - \delta_j) - B_{BUS,ij} \cos(\delta_i - \delta_j) \right)
\end{aligned}
$$

The MCM only interacts with MICs directly. The communication infrastructure supporting these interactions may consist of optical-fiber or power line communications. This optimization problem is also solved numerically in a centralized fashion.

C. System Operation Procedure

Based on the CERTS droop controllers, MICs, and MCM introduced in the current section and Section II, a typical system operation procedure is described, and information exchange relationships are also pointed out.

The system architecture is shown in figure 3. The MCM solves an optimization problem to maximize the real power injected by the consortium through primary substation into the main grid, while considering each microgrid's capacity, MV distribution line power flow constraints, and voltage regulation along the line. The solution to this optimization problem is a set of microgrid set points. These set points should be maintained at the PCC, between the microgrids and the MV distribution network. This set point serves as a constraint for the optimization problem solved by the MICs, with constraints concerning the microsource's capacity, line flow limits within the microgrid, and regulatory constraints on voltage and frequency. This optimization problem seeks to minimize the operational cost of the microgrid. Its output is a collection of voltage and real power set points in the microgrid. The lowest level controllers, i.e. CERTS droop controllers, use the real power and voltage set points as inputs, and actively adjust network frequency and reactive power to maintain voltage and frequency stability during operation.

When component parameters or network topologies change, the CERTS droop controllers should inform the MICs about the changes that have happened. After updating its system model, the MICs can recalculate set points for the CERTS controllers. Since the capacities of microgrids change, the solution to the MCM optimization problem must be updated to determine a group of new set points for the MICs.

V. Simulation Model

Both a preliminary and a complete simulation have been implemented in this section. With the basic five-bus network model, we conducted simulations to show the effectiveness of our control algorithm. It is shown that the operating condition determined by the MCM is maintained by the distribution network. Moreover, CERTS droop controller helps to maintain system stability under disturbances, without the need of communication between agents or higher level supervisors. We then incorporate the hierarchical controller into the network. To modify the previous model to implement the multi-layer control, each of the two farthest buses accommodates a Δ-connected microgrid, as shown in figure 15. Lines' parameters of the network are shown in table 1. This section also provides a comparison of simulation results with and without the MCM-MICs-CERTS control, indicating the benefit of implementing the hierarchical control algorithms.

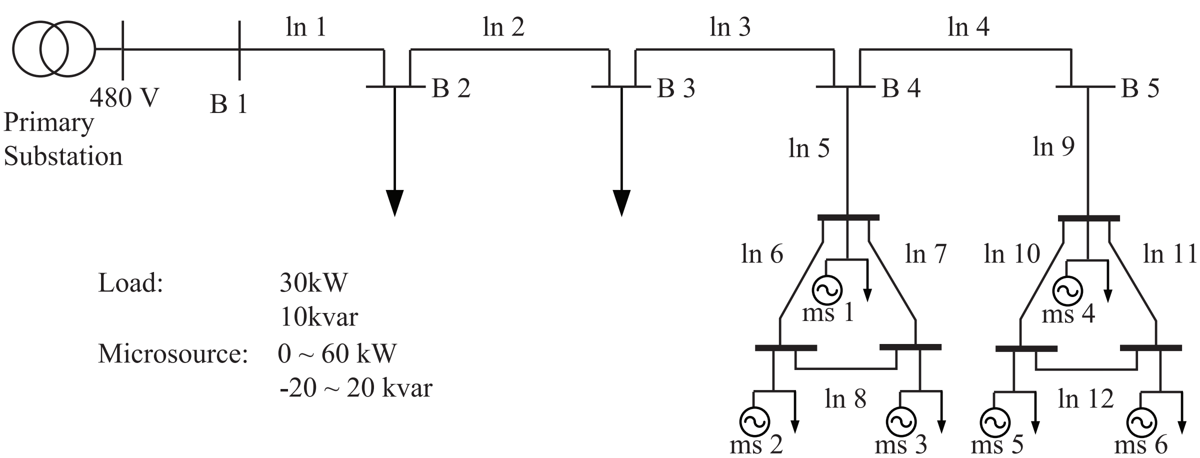

Figure 15. Microgrid Simulation Model Schematic Model

A. Preliminary Simulation

Based on the five-bus network model, we constructed a simulation model that incorporates a centralized controller to determine optimal set points for the two connected microsources. The distribution network

Table 1. Line Parameters of Distribution Network

Line	Type	Voltage (V)	Length (mile)	R (Ω)	X (Ω)
ln 1	AWG 1	480	1	0.786	0.156
ln 2	AWG 1	480	0.5	0.393	0.078
ln 3	AWG 1	480	0.5	0.393	0.078
ln 4	AWG 1	480	0.5	0.393	0.078
ln 5	AWG 1	480	0.2	0.1572	0.0312
ln 6	AWG 4	480	0.2	0.316	0.035
ln 7	AWG 4	480	0.2	0.316	0.035
ln 8	AWG 4	480	0.2	0.316	0.035
ln 9	AWG 1	480	0.2	0.1572	0.0312
ln 10	AWG 4	480	0.2	0.316	0.035
ln 11	AWG 4	480	0.2	0.316	0.035
ln 12	AWG 4	480	0.2	0.316	0.035

is working on $480V$ voltage level, with two loads tied to bus 2 and 3 and two microsources connected to bus 4 and 5. The loads both consume $30kW$ real power and $10kvar$ reactive power. The two microsources have a real power capacity between $0kW$ and $60kW$, and a reactive power capacity between $-20kvar$ and $20kvar$. The distribution line parameters correspond to ln 1, ln 2, ln 3, and ln 4 in table 1. Solving the optimization problem, we can determine set points for the two microsources to export maximum real power. The simulation model is shown in figure 16. The MCM block designates set points for both microsources. Each microsource is controlled by a CERTS droop controller. Its structure is illustrated in figure 7.

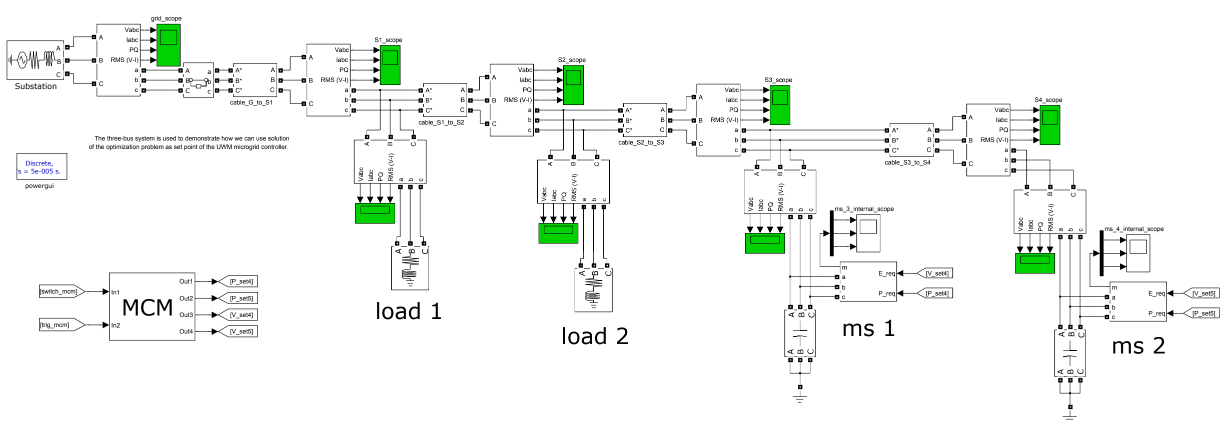

Figure 16. Preliminary Simulation Model

The solution to the MCM optimization problem matches with the simulation result, as shown in figure 17. The control inputs to the microsources are $P_{req} = 60kW$ and $E_{req} = 1.0344pu$ for "ms 1", $P_{req} = 14.43kW$ and $E_{req} = 1.0400pu$ for "ms 2". The resultant voltage magnitude, real and reactive power of each bus are identical in these two cases. The real power exported is about $4kW$, and the reactive power support required is around $62kvar$. Voltage magnitudes of all the five buses satisfy regulatory rules, and microsources' power outputs conform to their capacities. For comparison purposes, we also try to set E_{req} of the two microsources to be 1.0 pu. Even though more reactive power is supplied by the main grid, voltages of the two load buses violate the lower limit of voltage magnitude. As a result, the MCM is effective in controlling the coupled microgrids to achieve optimal operation.

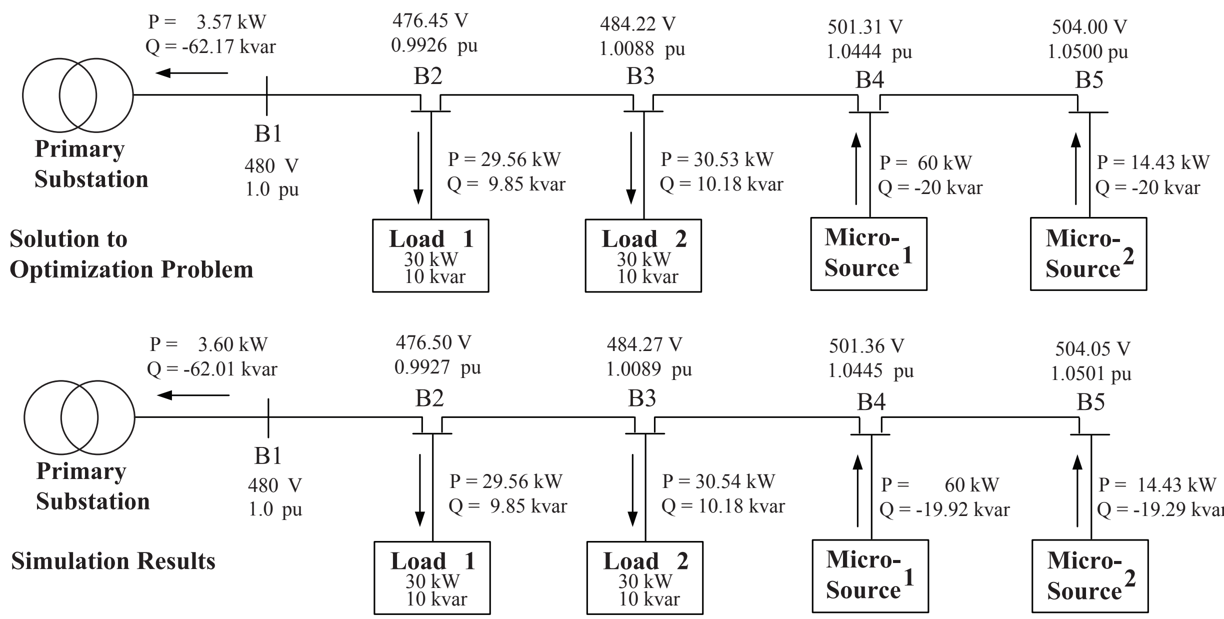

	ms 1	ms 2
P_{req}	60 kW	14.43 kW
E_{req}	1.0344 pu	1.0400 pu

Figure 17. Result of Preliminary Simulation Model

Under disturbances, the CERTS droop controllers by themselves are capable of keeping system stable, even without either communication among agents or higher level supervisors. We may, however, not be able to guarantee optimal system state, or have all the constraints satisfied. To return to optimal operation, MCM must recalculate set points so that maximum real power is exported while constraints being satisfied. The case of losing "load 2" is simulated during system operation, and the results with and without MCM recalculating set points are shown in figure 18.

Without the MCM, system stability is maintained during simulation and a steady state is achieved. Set points for the two microsources of voltage and real power are unchanged. Regulatory rules on voltage are violated on "bus 4" and "bus 5" both by about $0.01pu$. Microsource reactive power capacity are also exceeded on these two buses, since the reactive powers demanded by "ms 1" and "ms 2" are $26kvar$ and $21kvar$ larger than their capacities. At "bus 1", although $14kW$ more real power is exported to the main grid, almost

40$kvar$ more reactive power support is required by the network. This increased amount of reactive power support is not favorable in power grid.

In contrast, with MCM, the system regain its optimal state under the new circumstance. The operating condition respects all constraints considered in the MCM optimization problem. Set points of the two microsources are recalculated based on new parameters. Voltages on "bus 4" and "bus 5" are both 1.05pu, within limits. The real power export of "ms 1" and "ms 2" decrease by about 13kW and 10kW, while reactive power supports both lie within capacities of the microsources. At "bus 1", compared with the case without disturbances, the real power exported is 9kW more and the reactive power support needed is 11$kvar$ less. As a result, with MCM, not only system stability is maintained, but an optimal operation is also achieved. All constraints considered by the MCM optimization problem are satisfied automatically, and the reactive power demanded from the main grid is reduced.

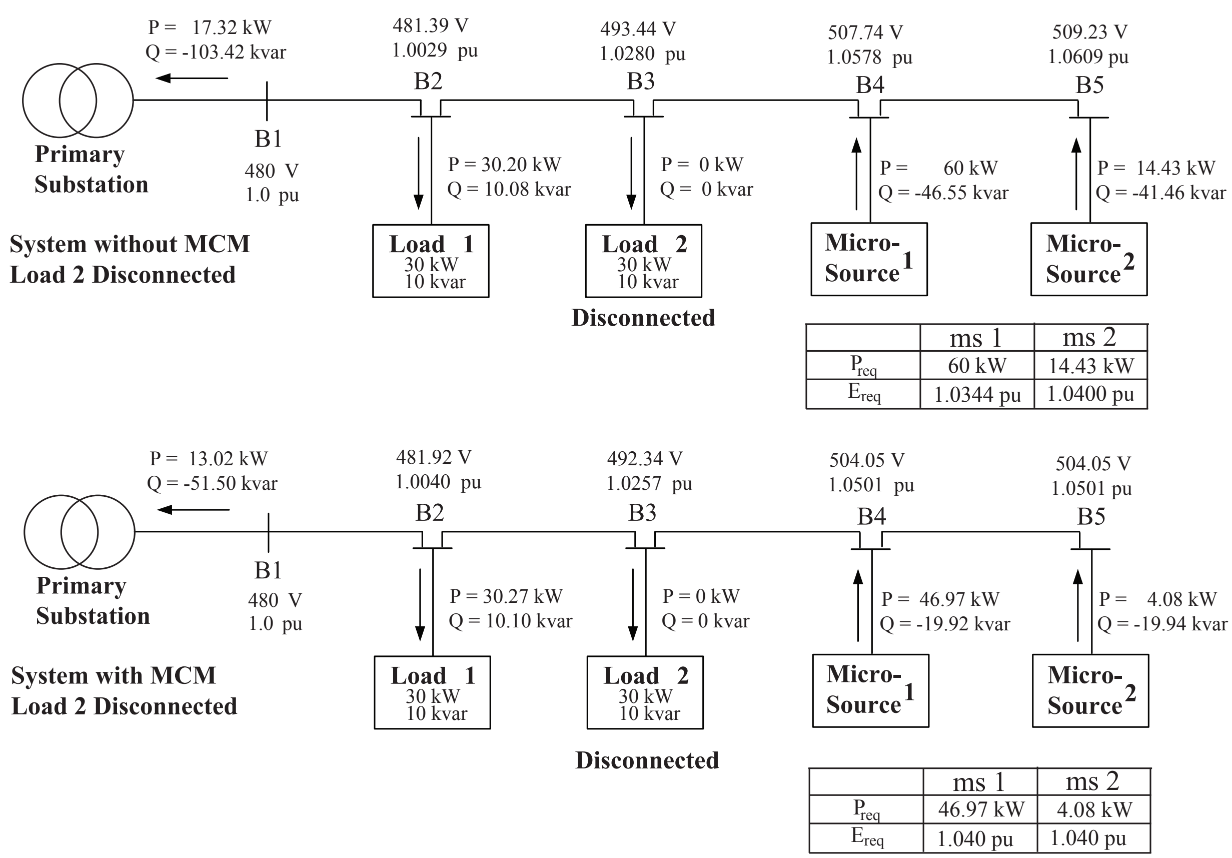

Figure 18. Comparison of single layer simulation results

B. Complete Simulation

The complete simulation model is shown in figure 19. In order to make sure the set points designated by the MCM are achievable for microgrids, we reduce real power capacity to between $0kW$ and $20kW$ and reactive power capacity to between $-20kvar$ and $10kvar$. The MCM determines the set points for the two microgrids, and each connected MIC determines set points for all microsources within its own microgrid. So the MCM block only designates set points to the MICs of the two microgrids, and the MIC blocks send commands to each CERTS droop controller. At each bus within a microgrid, besides the same microsource connected as above, a load is consuming $30kW$ real power and $10kvar$ reactive power. At "PCC 1" and "PCC 2", voltage regulatory rules must also be satisfied by controlling real and reactive power flows within microgrids. This power flow control is achieved by CERTS droop controllers connected to the microsources.

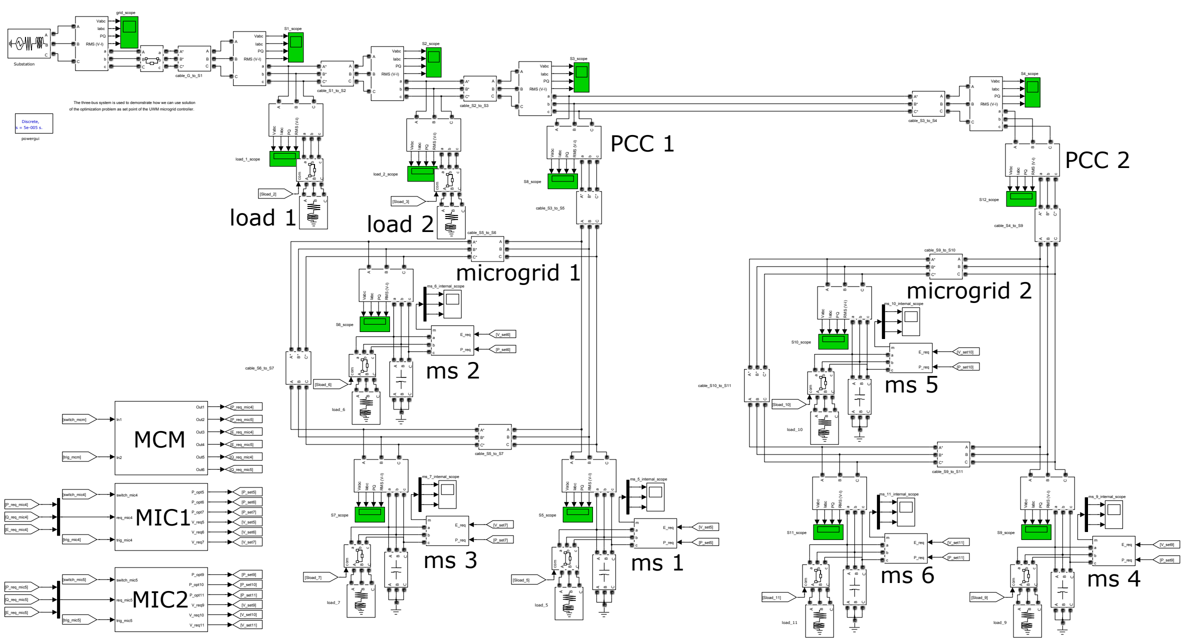

Figure 19. Complete Simulation Model

In figure 20, it is shown that optimal operation is achieved by the simulation model with corresponding set points. The set points for the microsources are listed at the bottom of the figure. The real power consumed by the network is about $19kW$, and the reactive power demand is around $13kvar$. Voltage magnitudes of all the buses are within the regulatory limits, and the microsources' power outputs conform to their capacities. For comparison purposes, the E_{req} of each microsource is set to $1.0pu$. With a similar amount of real power consumption, this case requires $40kvar$ more reactive power supplied by the main grid. This increased reactive power demand is not favorable in the power grid. As a result, our hierarchical controller is capable of controlling the coupled LV microgrids to export maximum real power, while satisfying constraints such as regulatory rules on voltage and frequency, MV and LV line power limits, as well as microsources' capacities.

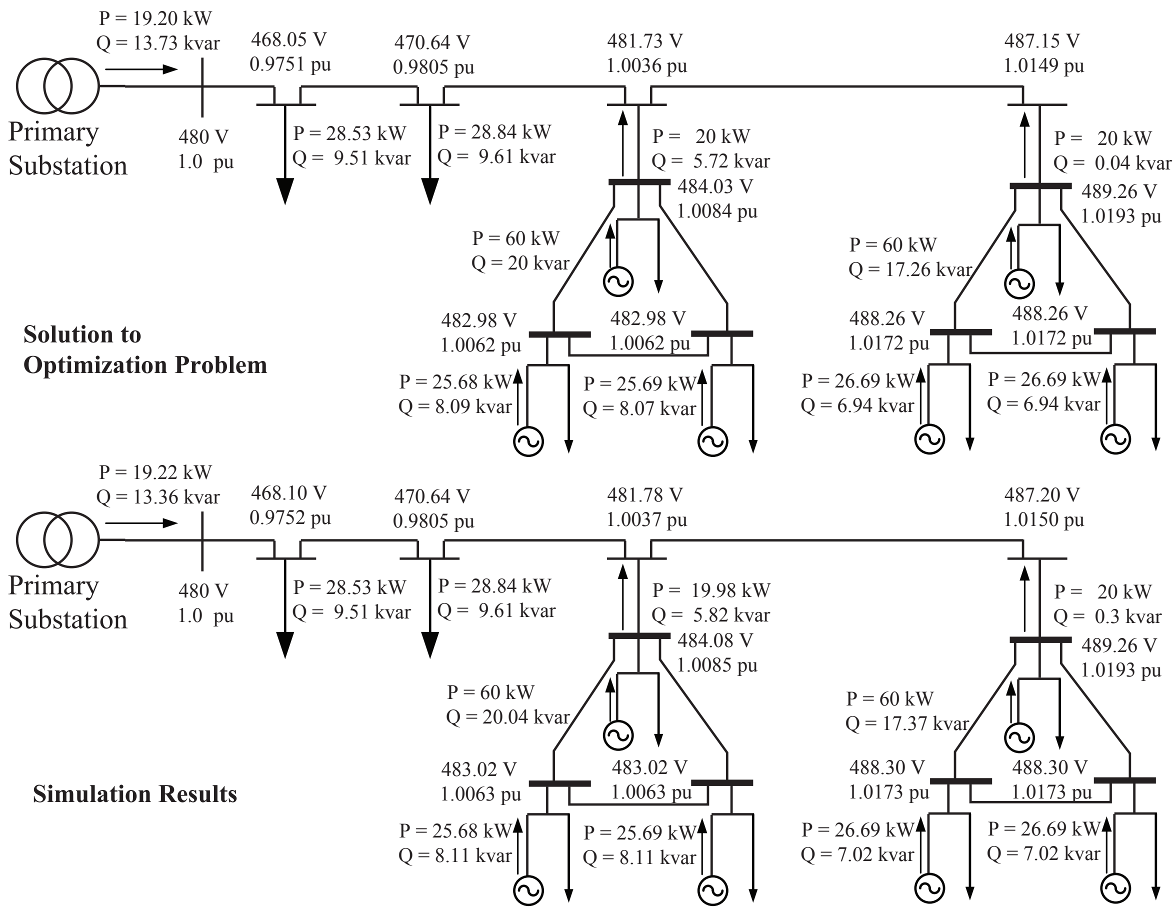

	ms 1	ms 2	ms 3	ms 4	ms 5	ms 6
P_{req}	60 kW	25.68 kW	25.69 kW	60 kW	26.69 kW	26.69 kW
E_{req}	1.0184 pu	1.0102 pu	1.0102 pu	1.0280 pu	1.0207 pu	1.0207 pu

Figure 20. Simulation Result of Complete Model

In case of disturbances, we can generally maintain system stability with only low level CERTS droop controllers. We can, however, use the proposed control architecture to return to an optimal state. The load on "bus 5" disconnects, and system performances are compared with and without the hierarchical control architecture. In both cases, system operates in acceptable states, but the amount of reactive power support from main grid increases substantially if the MCM-MIC-CERTS control structure is not used. With set point recalculations by the MCM and MICs, the impact of the load change to the entire system is greatly reduced. Simulation results are illustrated in figure 21.

Without the MCM and MICs, system stability is still maintained during simulation and a steady state is achieved. Regulatory rules on voltage are satisfied on all buses in the network, and microsource reactive power capacities are also respected. At "bus 1", although $10kW$ less real power is consumed by the network, the reactive power support demanded increases by the almost $80kvar$. This increased amount of reactive power support is not favorable during operation of the MV distribution network.

In contrast, with MCM-MIC-CERTS control architecture, the system regain its optimal state under the new circumstance. The system state respects all constraints considered in both the MCM and the MIC optimization problems. Set points of the microsources are recalculated based on new parameters. Compared with the case without disturbances, the set points of microsources within "microgrid 2" are unchanged. Because "load 5" is within "microgrid 1", those three microsources change their set points to adjust to the load disconnection. From "bus 1" to "bus 5", however, we have almost the same voltage profile and power flow situations for with and without disturbance situations. The impact of disturbances is isolated inside the microgrid, so that states at the PCCs are maintained. At "bus 1", the real and reactive power demands are kept to be about $19kW$ and $13kvar$. As a result, with MCM-MIC-CERTS controller structure, not only system stability is maintained, but an optimal operation is also achieved.

VI. Conclusion and Future Work

A hierarchical controller is proposed to achieve the objective of maximizing real power export from coupled LV microgrids to MV distribution network. The controller architecture is composed of, from bottom up, CERTS droop controllers for microsources, microgrid interface controllers (MICs) for microgrids, and a microgrid consortium manager (MCM). CERTS droop controllers are capable of maintaining system stability in an distributed fashion. MICs and the MCM determine set points based on corresponding optimization problems respectively. Constraints are respected as well, such as microsource capacity constraints, MV and LV line flow constraints, and regulatory rules on voltage and frequency. As shown in simulation results, we have solved the voltage rise problem when coupled LV microgrids export maximum real power back to the MV distribution network. Moreover, the control architecture deals with disturbances seamlessly, and regain optimal system operation. Based on our assumptions on distribution line properties, the control algorithm can work with MV and LV distribution networks, where real and reactive power controls are coupled together.

As far as future work is concerned, the proposed control algorithm needs to be verified to work compatibly with legacy control devices. This verification task would be accomplished based on our current simulation model built with SimPowerSystems^{TM} toolbox. Models of legacy equipments need to be built, as well as algorithms corresponding to DSO's regulation mechanisms. This part of project objective should be finished by January of 2012. Further, if time allows, we are interested in obtaining conditions to ensure system stability under particular set point situations. However, this part is not included in the main goal of this

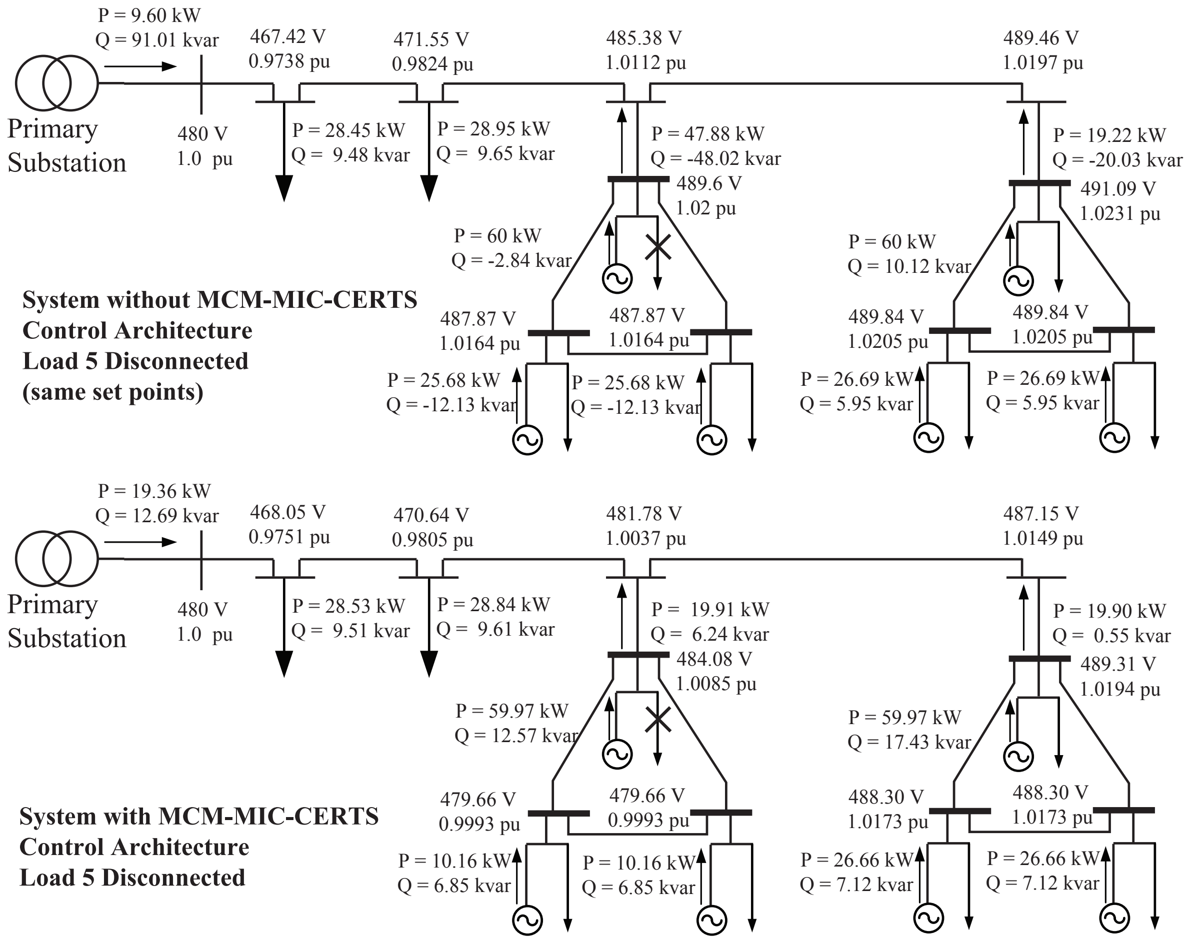

	ms 1	ms 2	ms 3	ms 4	ms 5	ms 6
P_{req}	60 kW	10.19 kW	10.19 kW	60 kW	26.69 kW	26.69 kW
E_{req}	1.0146 pu	1.0026 pu	1.0026 pu	1.0280 pu	1.0207 pu	1.0207 pu

Figure 21. Comparison of Performances with and without MCM-MIC-CERTS Control Architecture

project.

References

[1]Lasseter, R.H.; , "Smart Distribution: Coupled Microgrids," Proceedings of the IEEE , vol.99, no.6, pp.1074-1082, June 2011 doi: 10.1109/JPROC.2011.2114630.

[2]Masters, C.L.; , "Voltage rise: the big issue when connecting embedded generation to long 11 kV overhead lines," Power Engineering Journal , vol.16, no.1, pp.5-12, Feb. 2002 doi: 10.1049/pe:20020101.

[3]Hirst, E.; Kirby, B.;, "Electric-Power Ancillary Services," Oak Ridge National Laboratory, Feb. 1996 ORNL/CON-426.

[4]"Promotes Wholesale Competition through Open Access and Non-Discriminatory Transmission Service by Public Utilities," Federal Energy Regulatory Commission, RM95-8-000.

[5]Lasseter, R.; Piagi, P.; , "Control and Design of Microgrid Components," University of Wisconsin-Madison, January 2006.

[6]Engler, I.A.; , "International journal of distributed energy resources," International Journal of Distributed Energy Resources, Volume1 Number 1, Jan-Mar. 2005.